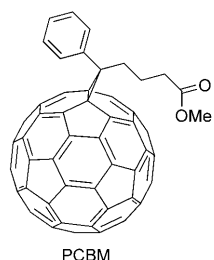


# Outstanding Short-Circuit Currents in BHJ Solar Cells Based on NIR-Absorbing Acceptor-Substituted Squaraines\*\*

Ulrich Mayerhöffer, Kaja Deing, Katrin Gruß, Holger Braunschweig, Klaus Meerholz,\* and Frank Würthner\*

In view of increasing global energy demand and finite resources of fossil fuels, photovoltaic devices are receiving a great deal of attention. Solution-processable organic semiconductors represent a promising class of new organic photovoltaic (OPV) materials with potential for low manufacturing costs and applications ranging from flexible and mobile devices to large-area installations.<sup>[1]</sup> In the best devices constructed to date based on solution-processed organic materials, interpenetrating networks of soluble n-type semiconducting fullerenes such as [6,6]-phenyl-C<sub>61</sub>-butyric acid methyl ester (PCBM) as electron acceptor and p-type semiconducting polymers such as poly(3-hexylthiophene) (P3HT) as electron donor moiety form the active interfaces. Such bulk heterojunction (BHJ) OPV cells have reached power conversion efficiencies (PCEs) of up to 6%.<sup>[2]</sup> Despite their still lower PCE of around 4%, solution-processable small-molecule-based BHJ solar cells are becoming increasingly attractive.<sup>[3]</sup> Owing to their simple purification and accessibility, paired with their mono-



dispersity and ease of modification, small p-type organic semiconductor molecules have overcome many drawbacks associated with their polymer pendants.<sup>[4]</sup> While established p-type organic semiconductor molecules, for example, oligothiophenes,<sup>[3a,b]</sup> triarylamine,<sup>[3c]</sup> and acenes,<sup>[3d]</sup> were

employed in initial BHJ cells of this type, recently traditional colorants such as merocyanines,<sup>[5a]</sup> squaraines,<sup>[5b]</sup> and dipyrromethene boron difluoride (BODIPY)<sup>[5c]</sup> dyes have been introduced, achieving PCE values of up to 1.7%. As such chromophore-based materials can be easily optimized, particularly in regard to absorbance in the highly desired red and near infrared (NIR) spectral region where the solar photon flux culminates,<sup>[6]</sup> improvement of tandem devices<sup>[2a]</sup> and realization of transparent photovoltaic systems as demanded for the application on window glass are further opportunities that might arise from such small-molecule NIR-absorber materials.

Squaraine dyes are a particularly promising class of chromophores for NIR OPV cells. They exhibit sharp and intense absorption bands in the desired long-wavelength region and possess considerable photo- and thermal stability under ambient conditions.<sup>[7]</sup> Thus, squaraines are a widely used class of functional dyes for a huge variety of applications.<sup>[8]</sup> Squaraines have been used in single-layer OPVs and, more recently, in vacuum-deposited and dye-sensitized solar cells.<sup>[9]</sup> Lately, Silvestri et al. reported for the first time on the use of squaraines in solution-processable BHJ solar cells with PCEs of up to 1.2%.<sup>[5b]</sup>

Herein we report on a series of squaraine dyes **5a–e** (Scheme 1) bearing an additional dicyanovinyl acceptor moiety at the central acceptor unit; these species afford solution-processed BHJ solar cells with PCEs of up to 1.79%. More importantly, absorption in the highly desired NIR range and short-circuit current densities up to  $J_{SC} = 12.6 \text{ mA cm}^{-2}$  are achieved with these squaraines. To our knowledge, this  $J_{SC}$  value is the highest reported for a small-molecule-based BHJ solar cell,<sup>[3,5]</sup> and compares favorably to  $J_{SC}$  of the currently best performing polymer-based BHJ solar cells.<sup>[2]</sup>

Squaraines **5a–e** and reference squaraines **7a,b** were synthesized according to the route outlined in Scheme 1.<sup>[10]</sup> For each of these squaraines, a series of BHJ solar cells was manufactured by spincoating squaraine/PCBM solutions on ITO/PEDOT:PSS substrates and subsequent thermal vacuum deposition of Ca/Al cathode (ITO = indium tin oxide, PEDOT = poly(3,4-ethylenedioxythiophene), PSS = poly(styrene sulfonate)). The photovoltaic properties of these devices were determined under standard AM (air mass) 1.5 solar radiation. The characteristic performance values of the BHJ solar cells for the investigated dyes are given in Table 1.

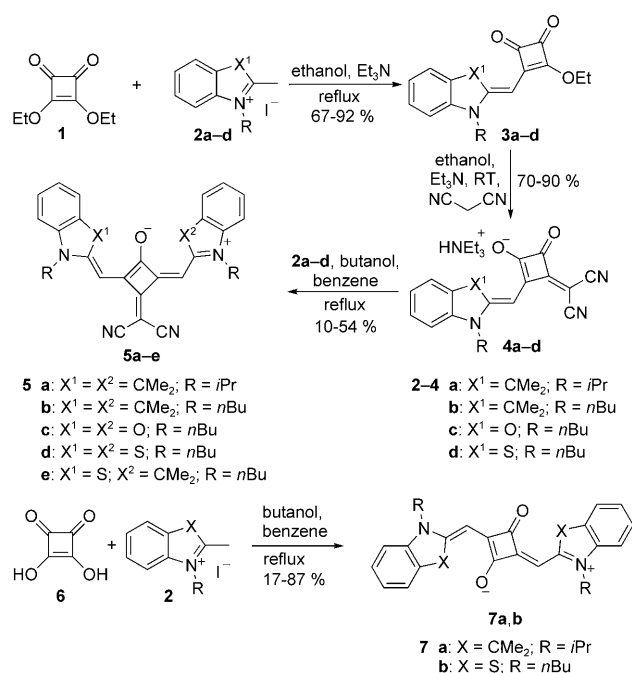
The devices based on the reference squaraines **7a,b** show low PCEs of 0.15 and 0.07%, respectively, at a squaraine/PCBM ratio of 3:7 (w/w), which turned out to be optimal within a concentration series. These poor efficiency values are accompanied by low short-circuit currents of around

[\*] U. Mayerhöffer, Prof. Dr. F. Würthner  
Universität Würzburg, Institut für Organische Chemie  
and  
Röntgen Research Center for Complex Material Systems  
Am Hubland, 97074 Würzburg (Germany)  
Fax: (+49) 931-318-4756  
E-mail: wuerthner@chemie.uni-wuerzburg.de  
K. Deing, Prof. Dr. K. Meerholz  
Department of Chemistry, Universität zu Köln  
Luxemburger Strasse 116, 50939 Köln (Germany)  
E-mail: klaus.meerholz@uni-koeln.de

K. Gruß, Prof. Dr. H. Braunschweig  
Universität Würzburg, Institut für Anorganische Chemie  
and  
Röntgen Research Center for Complex Material Systems  
Am Hubland, 97074 Würzburg (Germany)

[\*\*] Financial support by the DFG within priority program "Elementary processes of Organic Photovoltaics" is gratefully acknowledged. U.M. thanks the Fonds der Chemischen Industrie for a Ph.D. scholarship. BHJ = bulk heterojunction.

Supporting information for this article is available on the WWW under <http://dx.doi.org/10.1002/anie.200903125>.



**Scheme 1.** Synthesis of acceptor-substituted squaraines **5a–e** and reference squaraines **7a,b**.

**Table 1:** Electronic properties of the investigated squaraine dyes and the characteristic performance values for the respective BHJ solar cells with Ca/Al top electrode and a typical device thickness of about 80 nm.

Dye	$\lambda_{\text{max}}$ [nm] <sup>[d]</sup> ( $\epsilon_{\text{max}}$ [L mol <sup>-1</sup> cm <sup>-1</sup> ])	$E_{1/2}(\text{Ox})$ [V] <sup>[d]</sup>	$E_{\text{HOMO}}$ [eV] <sup>[e]</sup>	$E_{\text{LUMO}}$ [eV] <sup>[f]</sup>	wt % PCBM	$V_{\text{OC}}$ [V]	$J_{\text{SC}}$ [mA cm <sup>-2</sup> ]	$FF$ <sup>[g]</sup> [%]	PCE [%]
<b>7a</b> <sup>[a]</sup>	646 (250 000)	0.013	-5.16	-3.24	70	0.44	1.08	0.31	0.15
<b>7b</b> <sup>[b]</sup>	685 (210 000)	-0.167	-4.98	-3.17	70	0.22	1.02	0.30	0.07
<b>5a</b> <sup>[b]</sup>	683 (185 000)	0.101	-5.25	-3.42	70	0.63	3.28	0.36	0.74
<b>5b</b> <sup>[b]</sup>	683 (195 000)	0.120	-5.27	-3.45	70	0.66	3.49	0.37	0.84
<b>5c</b> <sup>[b]</sup>	625 (142 000)	0.009	-5.16	-3.18	40	0.42	2.79	0.42	0.49
<b>5d</b> <sup>[b]</sup>	701 (170 000)	-0.013	-5.14	-3.37	40	0.31	12.6	0.47	1.79
<b>5e</b> <sup>[b]</sup>	688 (180 000)	0.015	-5.17	-3.37	70	0.54	3.00	0.39	0.64

[a] Best device for squaraine/PCBM blend as cast. [b] Best device for squaraine/PCBM blend after annealing at 110°C for 15 min. [c] UV/Vis measurements in CH<sub>2</sub>Cl<sub>2</sub> solutions ( $c = 10^{-5}$  M). [d] Determined by cyclic voltammetry calibrated against the ferrocene/ferrocenium redox couple. [e]  $E_{\text{HOMO}} = -5.15 \text{ eV} - E_{\text{Ox}}$ ; [f]  $E_{\text{LUMO}} = E_{\text{HOMO}} + (hc/\lambda_{\text{max}})$ , see Figures S5–S8 in Supporting Information; [g]  $FF$  = fill factor.

1 mA cm<sup>-2</sup> and open-circuit voltages of  $V_{\text{OC}} = 0.44$  V for **7a** and  $V_{\text{OC}} = 0.22$  V for **7b**. It is worth mentioning that neither temperature nor duration of annealing has an influence on the device performance.

In contrast, the introduction of the dicyanovinyl functional group at the squaric acid unit in **5a** evoked a drastic (fivefold) increase in efficiency to a PCE value of 0.74% at the same squaraine/PCBM ratio of 3:7 (w/w). The open-circuit voltage and the short-circuit current of the device increased to  $V_{\text{OC}} = 0.63$  V and  $J_{\text{SC}} = 3.28$  mA cm<sup>-2</sup>. Similar values are obtained for **5b** with  $V_{\text{OC}} = 0.66$  V and  $J_{\text{SC}} = 3.49$  mA cm<sup>-2</sup>, resulting in a PCE value of 0.84%. For **5a** and **5b**, annealing at 110°C for 15 min enhances the PCE by about 10%. This improvement in PCE goes hand in hand with an increase in the short-circuit current, while the  $V_{\text{OC}}$  remains

nearly unchanged, suggesting that the annealing process leads to improved device morphology.<sup>[11]</sup>

The other acceptor-substituted squaraines **5c–e** also exhibit superior photovoltaic properties compared to those of **7a,b** (Table 1). In particular, squaraine **5d** features quite unique photovoltaic properties. While the reference compound **7b** shows the poorest performance, the corresponding dicyanovinyl-functionalized derivative **5d** exhibits a PCE of 1.79%, which is the highest of the present series. However, this good photovoltaic performance is only achieved upon annealing at 110°C for 15 min, which slightly reduces  $V_{\text{OC}}$  but strongly increases  $J_{\text{SC}}$ . This behavior again indicates dramatic changes in the device morphology.<sup>[11]</sup> The best performing devices for **5d** and **5c** were obtained for a squaraine/PCBM ratio of 6:4 (w/w). Such large optimum dye content is quite unusual for BHJ materials. It is, however, highly beneficial, because by increasing the proportion of squaraine in the active layer, more photons can be absorbed without increasing the layer thickness. These favorable material properties of **5d** manifest themselves in the short-circuit current density of  $J_{\text{SC}} = 12.6$  mA cm<sup>-2</sup> (Figure 1).

These high photocurrents are attributed to the presence of well-packed domains of PCBM and squaraine **5d** (for a discussion of packing properties, see below) that enable well-

balanced charge-carrier mobilities for electrons and holes. Indeed, thin films of **5d** exhibit appreciable hole-carrier mobility in organic field-effect transistors of  $\mu_{\text{h}} = 1.5 \times 10^{-5} \text{ cm}^2 \text{ V}^{-1} \text{ s}^{-1}$ , which further increases upon annealing to  $\mu_{\text{h}} = 1.3 \times 10^{-3} \text{ cm}^2 \text{ V}^{-1} \text{ s}^{-1}$  (for details, see the Supporting Information). Further evidence for the relatively high charge-carrier mobility of **5d** in the devices is given by the largest fill factor ( $FF$ ) of 47% within this series.<sup>[12]</sup>

From the above photovoltaic data it becomes evident that the

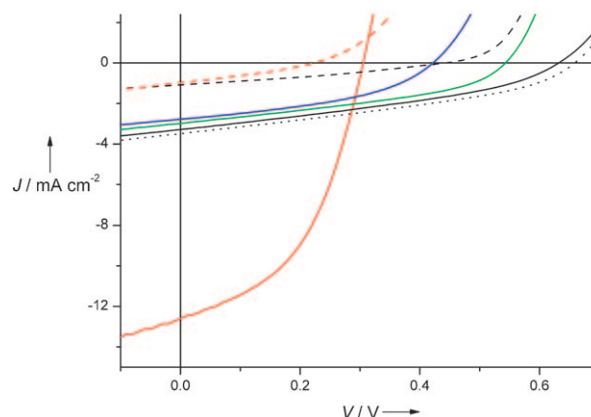


**Figure 1.**  $J$ - $V$  characteristics of **5a** (black solid line), **5b** (black dotted line), **5c** (blue solid line), **5d** (red solid line), **5e** (green solid line), **7a** (black dashed line), and **7b** (red dashed line) for the respective best solar cell devices measured under AM 1.5 illumination.

introduction of the dicyanovinyl moiety influences the molecular and material properties of squaraines to a great extent. The structural influence of this group is revealed by X-ray analysis of single crystals of **5a** and **5d** (see Figure 2 and

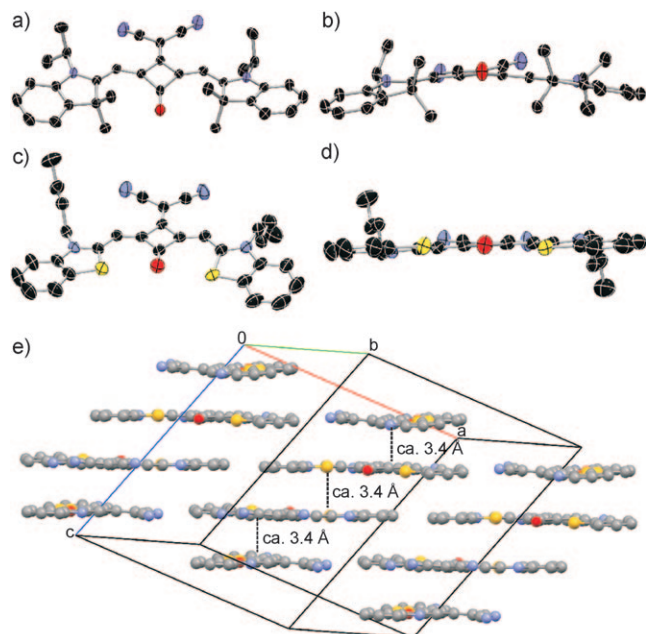


**Figure 2.** a) Molecular structure and b) front view of the squaraine plane of **5a**. c) Molecular structure and d) front view of the squaraine plane of **5d**. Thermal ellipsoids are set at the 50% probability level. Hydrogen atoms, the disorder of one alkyl chain in **5d**, and solvent molecules in **5a** are omitted for clarity. C black, N blue, O red, S yellow. e) Spatial arrangement of **5d** in the crystal lattice (for clarity, only the squaraine  $\pi$  system is shown).

the Supporting Information).<sup>[13]</sup> For the parent squaraines of the type **7a,b**, it was observed that the molecules are placed across an inversion center in the middle of the squarate ring with a *trans* arrangement of the donor groups, as shown in Scheme 1.<sup>[14]</sup> By introduction of the dicyanovinyl group, the inversion center is inevitably destroyed. Furthermore, the increased steric demand of the additional acceptor groups forces the donor groups into a *cis*-like arrangement.

Despite this mutuality, the structures of squaraines **5a** and **5d** also exhibit significant differences. Thus, the  $\pi$  backbone of squaraine **5a** is bent, with one indolenine ring in plane with the central squarate ring and the other one twisted out of the plane with a torsion angle of around  $12^\circ$  (Figure 2b). Furthermore, the dicyanovinyl unit is twisted about  $9^\circ$  relative to the plane of the squarate ring. Squaraine **5d**, in contrast, exhibits an almost planar  $\pi$  skeleton (Figure 2d).

This planarity allows squaraine **5d** to arrange in a densely packed “brickwork” arrangement with a closest interplanar distance of only 3.4 Å in the monoclinic space group *C2/c* (Figure 2e). This brickwork arrangement provides an excellent contact between the  $\pi$  systems, as demanded for efficient exciton and charge-carrier transport through the material. This beneficial arrangement explains the observed superior conductivity values<sup>[12]</sup> of **5d** compared to **5a**, whose bent

molecular structure inhibits such an advantageous spatial arrangement in the solid state.

The dicyanovinyl acceptor also favorably changes the absorption properties of compounds **5a–e** (Figure 3 and

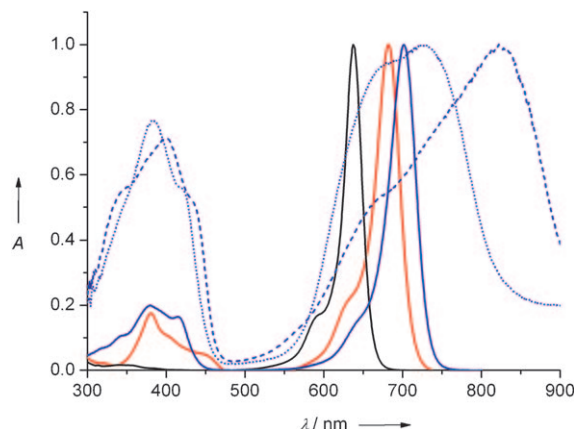


**Figure 3.** UV/Vis absorption spectra of squaraines **7a** (black solid line), **5a** (red solid line), and **5d** (blue solid line) in  $\text{CH}_2\text{Cl}_2$  ( $c = 10^{-5} \text{ M}$ ) and of **5d** in films (blue dotted line: as cast; blue dashed line: after annealing at  $110^\circ\text{C}$  for 15 min).

Figure S1–S4 in the Supporting Information). Reference dye **7a** shows a sharp and intense absorption band typical of symmetrical squaraines at 646 nm with an absorption coefficient of about  $\epsilon = 2.5 \times 10^5 \text{ M}^{-1} \text{ cm}^{-1}$ .<sup>[7b]</sup> The increased acceptor strength of the dicyanovinyl moiety in **5a** causes a red shift of the absorption maximum by about 40 nm to 683 nm ( $\epsilon = 1.85 \times 10^5 \text{ M}^{-1} \text{ cm}^{-1}$ ). Furthermore, a second absorption band with a maximum at 380 nm ( $\epsilon = 3.2 \times 10^4 \text{ M}^{-1} \text{ cm}^{-1}$ ) evolves. The same absorption characteristics are observed for all other acceptor-substituted squaraines (Table 1) and accordingly can be attributed to the molecular symmetry change of the dyes.

Owing to a pronounced excitonic coupling of these densely packed chromophores (Figure 2e), a substantial red shift and band broadening is observed in the solid state (dotted and dashed lines in Figure 3). Both of these spectral features are highly desirable, because they increase the absorption cross section for solar radiation and, eminently important for the application on window glass, expand the absorption far into the NIR region for the annealed film (Figure 3).<sup>[11]</sup> These beneficial properties manifest themselves in the external quantum efficiency (EQE). Thus, the **5d**/PCBM cell shows a maximum EQE of around 41 % at 750 nm, which belongs to the best EQEs reported for small-molecule-based BHJ cells (Figure S10 in the Supporting Information).

The only limitation for the efficient exploitation of solar irradiation arises from quite low open-circuit voltages, in particular for devices based on squaraines **7a,b** and **5c,d** (Table 1). One explanation for these low  $V_{\text{OC}}$  values comes from the rather high-lying HOMO energy levels of squaraines, which could be lowered by 0.1–0.2 eV by means of the dicyanovinyl substituents in derivatives **5a–e**. Another reason seems to be related to a strong interaction of these dyes in the

solid state that alters not only the optical properties but the frontier molecular orbital levels as well.<sup>[5a]</sup> It is, however, worth mentioning that the exploitation of the NIR spectral range always leads to a decrease of the utilizable excitation energy per absorbed photon, which is 3.1 eV at 400 nm but only 1.4 eV at 900 nm.

To conclude, we have achieved highly desired NIR-absorbing dyes for BHJ solar cells by a rational molecular engineering approach. Using these dyes, we could manufacture devices with PCEs up to 1.79 % and maximum  $J_{SC}$  values of  $12.6 \text{ mA cm}^{-2}$ ; the latter is the highest value reported for solution-processed small-molecule BHJ cells and is close to the  $J_{SC}$  values of the best polymer-based BHJ cells. Further investigations are currently underway to improve the device morphology and the electronic properties of the dyes towards higher  $V_{OC}$  values. Moreover, with their high  $J_{SC}$  in the NIR spectral range, **5d**/PCBM layers feature promising characteristics for application in tandem cell devices with established polymer-based materials such as P3HT/PCBM that exploit the shorter wavelength range of solar light.

Received: June 10, 2009

Published online: October 13, 2009

**Keywords:** bulk heterojunction solar cells · donor-acceptor systems · dyes/pigments · squaraines · thin films

- [1] a) R. M. Nault, *Basic Research Needs for Solar Energy Utilization—Report of the Basic Energy Sciences Workshop on Solar Energy Utilization*, April 18–21, **2005**; [http://www.sc.doe.gov/bes/reports/files/SEU\\_rpt.pdf](http://www.sc.doe.gov/bes/reports/files/SEU_rpt.pdf); b) C. J. Brabec, N. S. Sariciftci, J. C. Hummelen, *Adv. Funct. Mater.* **2001**, *11*, 15–26.
- [2] a) J. Y. Kim, K. Lee, N. Coates, D. Moses, T.-Q. Nguyen, M. Dante, A. J. Heeger, *Science* **2007**, *317*, 222–225; b) J. Peet, J. Y. Kim, N. E. Coates, W. L. Ma, D. Moses, A. J. Heeger, G. C. Bazan, *Nat. Mater.* **2007**, *6*, 497–500.
- [3] a) B. Walker, A. B. Tamayo, X.-D. Dang, P. Zalar, J. H. Seo, A. Garcia, M. Tantiwiwat, T.-Q. Nguyen, *Adv. Funct. Mater.* **2009**, *19*, 3063–3069; b) C.-Q. Ma, M. Fonrodona, M. C. Schikora, M. M. Wienk, R. A. J. Janssen, P. Bäuerle, *Adv. Funct. Mater.* **2008**, *18*, 3323–3331; c) M. T. Lloyd, A. C. Mayer, S. Subramanian, D. A. Mourey, D. J. Herman, A. V. Bapat, J. E. Anthony, G. G. Malliaras, *J. Am. Chem. Soc.* **2007**, *129*, 9144–9149; d) S. Roquet, A. Cravino, P. Leriche, O. Aleveque, P. Frere, J. Roncali, *J. Am. Chem. Soc.* **2006**, *128*, 3459–3466.
- [4] M. Brumbach, D. Placencia, N. R. Armstrong, *J. Phys. Chem. C* **2008**, *112*, 3142–3151.
- [5] a) N. M. Kronenberg, M. Deppisch, F. Würthner, H. W. A. Lademann, K. Deing, K. Meerholz, *Chem. Commun.* **2008**, 6489–6491; b) F. Silvestri, M. D. Irwin, L. Beverina, A. Facchetti, G. A. Pagani, T. J. Marks, *J. Am. Chem. Soc.* **2008**, *130*, 17640–17641; c) T. Rousseau, A. Cravino, T. Bura, G. Ulrich, R. Ziessel, J. Roncali, *Chem. Commun.* **2009**, 1673–1675.
- [6] M. M. Wienk, M. G. R. Turbiez, M. P. Struijk, M. Fonrodona, R. A. J. Janssen, *Appl. Phys. Lett.* **2006**, *88*, 153511.
- [7] a) D. Keil, H. Hartmann, T. Moschny, *Dyes Pigm.* **1991**, *17*, 19–27; b) S. Sreejith, P. Carol, P. Chithra, A. Ajayaghosh, *J. Mater. Chem.* **2008**, *18*, 264–274.
- [8] a) G. J. Ashwell, G. Jefferies, D. G. Hamilton, D. E. Lynch, M. P. S. Roberts, G. S. Bahra, C. R. Brown, *Nature* **1995**, *375*, 385–388; b) D. Ramaiah, I. Eckert, K. T. Arun, L. Weidenfeller, B. Epe, *Photochem. Photobiol.* **2002**, *76*, 672–677; c) K.-Y. Law, *Chem. Rev.* **1993**, *93*, 449–486; d) J. V. Ros-Lis, R. Martínez-Máñez, F. Sancenón, J. Soto, M. Spieles, K. Rurack, *Chem. Eur. J.* **2008**, *14*, 10101–10114.
- [9] a) D. L. Morel, A. K. Ghosh, T. Feng, E. L. Stogryn, P. E. Purwin, R. F. Shaw, C. Fishman, *Appl. Phys. Lett.* **1978**, *32*, 495–497; b) S. Wang, E. I. Mayo, M. D. Perez, L. Griffe, G. Wei, P. I. Djurovich, S. R. Forrest, M. E. Thompson, *Appl. Phys. Lett.* **2009**, *94*, 233304; c) J.-H. Yum, P. Walter, S. Huber, D. Rentsch, T. Geiger, F. Nüesch, F. De Angelis, M. Grätzel, M. K. Nazeeruddin, *J. Am. Chem. Soc.* **2007**, *129*, 10320–10321.
- [10] For synthetic details and compound characterization, see the Supporting Information.
- [11] For details on the device morphology, see the Supporting Information.
- [12] One limiting factor for BHJ cells is known to be the buildup of space charge, which may occur if the charge-carrier mobility difference between the donor and acceptor phase exceeds two orders of magnitude. Under this condition the  $FF$  value is less than 42 %, see: a) V. D. Mihailetschi, J. Wildeman, P. W. M. Blom, *Phys. Rev. Lett.* **2005**, *94*, 126602; b) L. J. A. Koster, V. D. Mihailetschi, P. W. M. Blom, *Appl. Phys. Lett.* **2006**, *88*, 052104.
- [13] CCDC 734983 (**5a**) and 734984 (**5d**) contain the supplementary crystallographic data for this paper. These data can be obtained free of charge from The Cambridge Crystallographic Data Centre via [www.ccdc.cam.ac.uk/data\\_request/cif](http://www.ccdc.cam.ac.uk/data_request/cif).
- [14] D. E. Lynch, K. A. Byriel, *Cryst. Eng.* **1999**, *2*, 225–239.